Kinetics of the Initial Steps of Rabbit Psoas Myofibrillar ATPases Studied by Tryptophan and Pyrene Fluorescence Stopped-Flow and Rapid Flow-Quench. Evidence That Cross-Bridge Detachment Is Slower than ATP Binding†

Robert Stehle,*,‡ Corinne Lionne,§ Franck Travers,§ and Tom Barman§

INSERM U128, IFR24, 1919 route de Mende, 34293 Montpellier Cedex 5, France, and Department of Vegetative Physiology, University of Köln, Robert-Koch-Strasse 39, 50931 Köln, Germany

Received March 1, 2000; Revised Manuscript Received April 24, 2000

ABSTRACT: The kinetics of the tryptophan fluorescence enhancement that occurs when myofibrils (rabbit psoas) are mixed with Mg-ATP were studied by stopped-flow in different solvents (water, 40% ethylene glycol, 20% methanol) at 4 °C. Under relaxing conditions (low Ca^{2+}) in water ($\mu = 0.16$ M, pH 7.4) and at high ATP concentrations, the transient was biphasic, giving a k^{fast}_{max} of 230 s^{-1} and a k^{slow}_{max} of 15 s^{-1}. The kinetics of the two phases were compared with those obtained by chemical sampling using [γ-^{32}P]-ATP and quenching in acid (P_i burst experiments: these give unambiguously the ATP cleavage kinetics), or cold Mg-ATP (cold ATP chase: ATP binding kinetics). k^{slow} is due to ATP cleavage, as with S1. Interestingly, k^{fast} is slower than the ATP binding kinetics. Instead, this constant appears to report ATP-induced cross-bridge detachment from actin because (1) it was identical to the fluorescence transient obtained on addition of ATP to pyrene-labeled myofibrils; (2) when the initial filament overlap in the myofibrils was decreased, the amplitude of the fast phase decreased; (3) there was no fluorescent enhancement upon the addition of ADP to myofibrils. This is different from the situation with S1 or actoS1 where there was also a fast fluorescent ATP-induced transient but whose kinetics were identical to those of the tight ATP binding. To increase the time resolution and to confirm our results, we also carried out transient kinetics in ethylene glycol and methanol. We interpret our results by a scheme in which a rapid equilibrium between attached (AM*·ATP) and detached (M*·ATP) states is modulated by the fraction of myosin heads in rigor (AM) during the time of experiment.

There is general agreement that in muscle contraction the chemical energy provided by the myosin head ATPase is converted into a cyclic interaction of this molecular motor with actin (*1*−*3*). A key problem in understanding this chemomechanical transduction is to correlate the different myosin ATPase intermediates with their actin-binding properties, but despite intensive investigations there remain several outstanding questions. Here we focus on the coupling between the myosin ATPase and acto−myosin interactions during the initial steps of myofibrillar ATPase.

A way to approach the problem is to work with myofibrils because with these both mechanical (*4*, *5*) and transient chemical kinetic experiments (*6*−*9* and references cited therein) are possible. The myofibril is a structurally organized system: it is the functional contractile unit of muscle that appears to be fully regulated (*10* and references cited therein). Further, their mechanical properties are very similar to those of muscle fibers (*5*).

Transient enzyme kinetics are studied principally by two techniques: optically by stopped-flow and chemically by the rapid quench flow method. With the myofibril, rapid quench flow has been the method of choice for two reasons. First, optical methods are difficult with turbid systems such as the myofibrils. Second, provided that a suitable analytical method is available, with the rapid flow-quench method, one can measure unambiguously the rates of formation and decomposition of a given chemical entity. This method is particularly useful when coupled with the use of radioactive substrates which ensures high specificity and sensitivity. Thus, with myofibrils most quench flow studies involve [γ-^{32}P]ATP and the measurement of [^{32}P]P_i.[1] However, the use of [γ-^{32}P]ATP suffers from the disadvantage that to keep the signal-to-noise ratio high, the [γ-^{32}P]ATP to myosin head molar ratio must be less than 20:1 which means that the ATP concentration is limited to less than 0.2 mM as it is difficult technically to work at high concentrations of myofibrils. This is well below the ATP concentrations needed to saturate certain of the processes on the myofibrillar ATPase and, of

† R.S. is grateful to INSERM for a fellowship and C.L. to the Association Française contre les Myopathies and the Société de Secours des Amis des Sciences for financial support.

* To whom correspondence should be addressed. Phone: 49 221 478 6952. Fax: 49 221 478 6965. E-mail: Robert.Stehle@Uni-Koeln.de.

‡ University of Köln.

§ INSERM U128.

[1] Abbreviations: DTT, dithiothreitol; EDTA, ethylenediaminetetraacetic acid; EGTA, ethylene glycol bis(β-aminoethyl ether)-*N*,*N*,*N*′,*N*′-tetraacetic acid; P_i, inorganic orthophosphate; PIPES, piperazine-*N*,*N*′-bis(2-ethanesulfonic acid); PMSF, phenylmethanesulfonyl fluoride; pyrene, *N*-(1-pyrenyl)iodoacetamide group; S1, myosin subfragment 1; Tris, tris(hydroxymethyl)aminomethane.

10.1021/bi0004753 CCC: $19.00
Published on Web 06/03/2000

course, those used in mechanical studies (several millimolar). Further, we do not have a method for investigating cross-bridge detachment rates in native myofibrils.

Experiments at high ATP concentrations are possible with the stopped-flow method. Further, this method is less laborious and expensive in material than the rapid quench flow method. There are two studies in which the myofibrillar ATPases have been studied optically. One is due to Ma and Taylor (*8*), who attached the fluorescent pyrinyl group to myofibrils. Upon the addition of ATP to pyrene-labeled myofibrils, there was a low but significant increase in fluorescence, and it was possible to study the kinetics of this by stopped-flow at millimolar concentrations of ATP. Previous work with pyrene-labeled actin in actoS1 had shown that the pyrene group reports actoS1 dissociation with kinetics directed by the ATP binding process (*11* and references cited therein). Ma and Taylor interpreted their results accordingly; however, there is uncertainty as to the location of the pyrene group in the multiprotein myofibril.

The other study is due to White (*7*) and is based on the intrinsic fluorescence properties of the myofibril. It had been known for a long time that when ATP is added to S1, there is an enhancement of tryptophan fluorescence which has been exploited to study the transient kinetics of the initial steps of the ATPases of S1 and actoS1 (*12*−*17*). White (*7*) showed that upon mixing manually myofibrils with ATP in a fluorometer, there was an enhancement of tryptophan fluorescence. Because of the slow mixing technique, the experiments were limited to low ATP concentrations, so the kinetics of the enhancement were interpreted as a reflection of the ATP binding process. This pioneering work encouraged us to undertake a detailed transient kinetic study that exploits the ATP-induced tryptophan fluorescence changes in myofibrils by stopped-flow, a study that was made possible by the availability of a high-quality fluorescence stopped-flow apparatus. The aims of our work were as follows: first, to identify the step(s) that contribute(s) to the fluorescence enhancement and thereby develop further methods to study the initial steps of the myofibrillar ATPase; second, to allow for experiments at high ATP concentration on native (chemically unmodified) myofibrils; and finally, to provide a model for kinetic studies on precious preparations such as biopsies (e.g., from patients suffering from familial hypertrophic cardiomyopathy) or genetically engineered material. A preliminary report of this work has been presented (*18*).

MATERIALS AND METHODS

Myofibrils, S1, and Chemicals. S1 was prepared as in Biosca et al. (*19*) and used within 2 days. Myofibrils were prepared from rabbit psoas muscle as in Herrmann et al. (*20*) and stored at 4 °C up to 3 days in storage buffer (0.1 M K-acetate, 5 mM KCl, 2 mM Mg-acetate, 50 mM Tris-acetate, 1 mM DTT, pH 7.4) to which 20 μg/mL sodium azide, 10 μg/mL PMSF, 2 μg/mL leupeptin, and 2 μg/mL pepstatin had been added.

Pyrene-labeled myofibrils were prepared as described by Ma and Taylor (*8*). *N*-(1-Pyrenyl)iodoacetamide in dimethyl sulfoxide was added to myofibrils at a 5:1 molar ratio (pyrene/actin) and reacted overnight at 4 °C in labeling buffer (25 mM PIPES, 100 mM NaCl, 2 mM $MgCl_2$, 1 mM EGTA, pH 7.0). The reaction was stopped by adding 2 mM DTT, and the myofibrils were immediately washed by two centrifugation steps (10 min at 3000*g* at 4 °C). The steady-state ATPases in the presence of Ca^{2+} or EGTA for pyrene-labeled myofibrils were the same as for the unlabeled myofibrils (results not shown).

Scheme 1

$$\mathrm{M + ATP} \overset{K_1}{\rightleftharpoons} \mathrm{M.ATP} \underset{k_{-2}}{\overset{k_2}{\rightleftharpoons}} \mathrm{M^*.ATP} \overset{k_3}{\underset{k_{-3}}{\rightleftharpoons}} \mathrm{M^{**}.ADP.Pi} \xrightarrow{k_4} \mathrm{M + ADP + Pi}$$

Myofibrils of different sarcomere lengths were prepared from fiber bundles mounted to wooden sticks that had been left overnight in rigor buffer (0.1 M K-acetate, 5 mM KCl, 5 mM EDTA, 50 mM Tris-acetate, 1 mM DTT, pH 7.4) according to the method of Knight and Trinick (*21*). The mean sarcomere lengths were determined before the experiments from 10−20 myofibrils using a Normaski microscope (Nikon Microphot equipped with a 100× objective).

Immediately before experimentation with myofibrils, any aggregates were removed by filtration through a polypropylene filter of 149 μm pore openings (Spectra Mesh, Spectrum Medical Industries, Inc., Laguna Hills, CA). The concentration of myosin heads was measured by the absorption at 280 nm (*22*).

Ethylene glycol and methanol (analytical grade) were from Merck, Darmstadt, Germany, and [γ-^{32}P]ATP was from Amersham International. The sources of the other chemicals are in Herrmann et al. (*20*) and Lionne et al. (*23*).

Experimental Buffers. The basic buffer was 0.1 M K-acetate, 5 mM KCl, 5 mM Mg-acetate, and 50 mM Tris adjusted to pH 7.4 at 20 °C with acetic acid with or without 40% (v/v) ethylene glycol or 20% methanol. For experiments in the absence of Ca^{2+}, the buffer contained 2 mM EGTA; these conditions are referred to as "relaxed". For those in the presence of Ca^{2+} ("activated"), it contained 0.1 mM $CaCl_2$.

Rapid Flow-Quench Experiments. These were carried out in a home-built, thermostatically controlled rapid flow-quench apparatus (*24*). This is a point by point method in which reaction mixtures are quenched at times *t* and the quenched reaction mixtures analyzed. It has been used with myosin, actomyosin, and myofibrillar ATPases under different sets of conditions. Here we carried out two types of experiment with S1 and myofibrils, and as a first approach, we interpreted our data by Scheme 1 where M represents myosin heads with or without actin.

In *cold ATP chase experiments*, the reaction mixtures (S1 or myofibrils plus [γ-^{32}P]ATP) were first quenched in a large excess (330-fold) of unlabeled ATP in the apparatus, incubated on ice for 3 min, and then finally quenched in 22% trichloroacetic acid + 1 mM KH_2PO_4, and $^{32}P[P_i]$ was determined by the filter paper method of Reimann and Umfleet (*25*). Since in Scheme 1 step 2 is essentially irreversible, one obtains a single exponential transient phase of tight binding of ATP of kinetics $k_{obs} = k_2[ATP]/(K_1 + [ATP])$ and amplitude equal to the ATPase site concentration.

In *P_i burst experiments*, reaction mixtures are quenched directly in acid, and $^{32}P[P_i]$ is determined. Here we obtain a transient burst phase of P_i (representing enzyme-bound as well as free P_i) of kinetics $(k_2/K_1)[ATP]$ at low [ATP] and $k_3 + k_{-3}$ at high [ATP].

Fluorescence Stopped-Flow Experiments. These were carried out in a High Tech Scientific stopped-flow apparatus

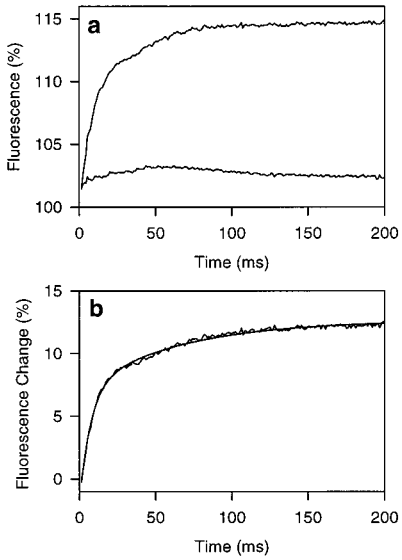

FIGURE 1: Analysis of the ATP-induced tryptophan fluorescence transients in relaxed myofibrils as observed by stopped-flow at 4 °C. (a) Typical records obtained by mixing myofibrils with buffer alone (lower trace) or high [ATP] (upper trace). The reaction mixture was 3 μM in myosin heads plus 1 mM ATP. The buffer was 0.1 M potassium acetate, 5 mM magnesium acetate, 2 mM EGTA, and 50 mM Tris-acetate, pH 7.4. (b) Corrected trace obtained by subtracting the signal without ATP from that with ATP. The curve was fitted to two exponentials: a fast phase of amplitude = 9.1% and kinetics $k^{\text{Trp fast}} = 136\ \text{s}^{-1}$ and a slow phase of amplitude = 5.5% and kinetics $k^{\text{Trp slow}} = 15.3\ \text{s}^{-1}$. For further details, see Materials and Methods.

(model SF-61 DX2) which was particularly well adapted to our UV fluorescence measurements. To measure the tryptophan fluorescence, the excitation wavelength was 295 nm and emission was ≥320 nm; for the pyrene fluorescence, excitation = 365 nm, emission ≥ 399 nm. For each experimental condition, a series of 3−12 shots was performed and averaged. Just before an experiment, the fluorescence of the myofibrillar solution in the stopped-flow cell (without ATP) was set as 100%. The correction for the dead time of the apparatus (1.7 ms) was made automatically by the Hi-Tech system.

Figure 1a shows typical mean signals obtained by mixing a suspension of myofibrils with buffer with or without ATP. Merely diluting a suspension of myofibrils with buffer in the stopped-flow cell leads to a small background signal: a transient increase (about 1% of total fluorescence in the first 100 ms), followed by a decrease (about 1% in the seconds time range), and a drift due to photobleaching (a decrease of typically 1−2% per minute). To compensate for these artifacts, from each mean signal obtained from experiments in the presence of ATP, a corresponding mean of the background signals obtained at the same experimental conditions but without ATP was subtracted. This difference signal of these means (Figure 1b) was then fitted by either one or two exponentials (depending upon the ATP concentrations) to obtain the kinetic parameters.

The amplitude of the fluorescence signals depended on the homogeneity of the preparation. In particular, filtration of the myofibrillar suspensions was important to obtain high amplitudes of the fluorescence signal. Attempts to measure fluorescence transients and spectroscopic changes in a fluorometer by mixing myofibrillar suspensions with ATP by hand failed because despite continuous stirring myofibrils formed loose cloudy aggregates in the cuvette. The fast mixing provided by the stopped-flow apparatus favors a homogeneous dispersion of myofibrils which is necessary for obtaining reproducible fluorescence signals.

Kinetic Data Analysis and Simulation. Stopped-flow records were fitted directly by the KinetAsyst program of Hi-Tech to single or double exponentials which gave kinetic constants and amplitudes. In the same way, the rapid flow-quench data were fitted by GraFit (Erithacus Software) or Sigmaplot (Scientific Graphing Software). The dependences of k_{obs} on the ATP concentration were generally hyperbolic and fitted, with the same programs, to the function $(k_{\text{obs max}} \times [\text{ATP}])/(K_{0.5} + [\text{ATP}])$. The meaning of $K_{0.5}$ depends on the type of experiments.

Simulations, carried out with Microsoft Excel 97, were based on Scheme 2 with $K_T = k_-/k_+$. For both these rate constants, a dependence on the rigor fraction ($[\text{A}-\text{M}]/[\text{M}_{\text{total}}]$) was defined, which was then used in the simulations to calculate K_T and fractions of detached states at time t based on the fraction of A−M (R) at time t. R was assumed to be 1 at $t = 0$ and to decay exponentially with a rate constant of $k_2[\text{ATP}]/(K_1 + [\text{ATP}])$ to 0 at $t = \infty$. Thus, the chase signal was calculated by $1 - R(t)$. The fluorescence signal (fast myofibrillar tryptophan fluorescence or pyrene signals) was calculated by $[1 - R(t)]\{k_-(t)/[k_+(t) + k_-(t)]\}$. The P_i burst signal was calculated stepwise by $[\text{A}\sim\text{M}^{**}\cdot\text{ADP}\cdot\text{P}_i](t_i) = [\text{A}\sim\text{M}^{**}\cdot\text{ADP}\cdot\text{P}_i](t_{i-1}) + (\text{fluorescence signal} - [\text{A}\sim\text{M}^{**}\cdot\text{ADP}.\text{P}_i] \times (t_{i-1}))k_3(t_i - t_{i-1}) - [\text{A}\sim\text{M}^{**}\cdot\text{ADP}\cdot\text{P}_i](t_{i-1})k_{-3}(t_i - t_{i-1})$. The steps following the cleavage were not included in the simulations, which therefore gave transient kinetics only and not steady-state rates.

We have already discussed the problems of the quality of fits and errors (*9*).

RESULTS

Myofibrillar Tryptophan Fluorescence Enhancement with ATP in Aqueous Buffer. Figure 2a shows transients obtained by mixing myofibrils with Mg-ATP at various concentrations in the absence of Ca^{2+}, at 4 °C.

At low ATP concentrations (≤50 μM), there was a lag phase in the signal, followed by a burst. As a first approximation, we ignored the lag, and we fit the burst phase with a single exponential of kinetics k_{obs}. The kinetics of both phases increased with an increase in the ATP concentration. We note that whereas transient lag phases were obtained in the fluorescence signals, none was detected in ATP chase experiments (*26*).

At ATP concentrations ≥250 μM, the lag phase was no longer observed on the time scale of the experiments. The burst phase became biphasic, and by fitting it to two exponentials, we obtained constants for fast ($k^{\text{Trp fast}}$) and slow ($k^{\text{Trp slow}}$) phases. The ATP dependences of $k^{\text{Trp fast}}$ and $k^{\text{Trp slow}}$ are shown in Figures 2c and 2d. $k^{\text{Trp slow}}$ appears to be independent of the ATP concentration up to 3 mM with a value of $15 \pm 3\ \text{s}^{-1}$ (Figure 2d). This is close to the $18 \pm 2\ \text{s}^{-1}$ obtained for the P_i burst kinetics ($k_3 + k_{-3}$ in Scheme 1) at 45 μM ATP under identical conditions (*26*). The $k^{\text{Trp fast}}$ versus [ATP] dependence fit to an hyperbola, giving a $K_{0.5}$ of approximately 740 ± 140 μM and a maximum value of $230 \pm 30\ \text{s}^{-1}$ (Figure 2c). These results are summarized in Table 1.

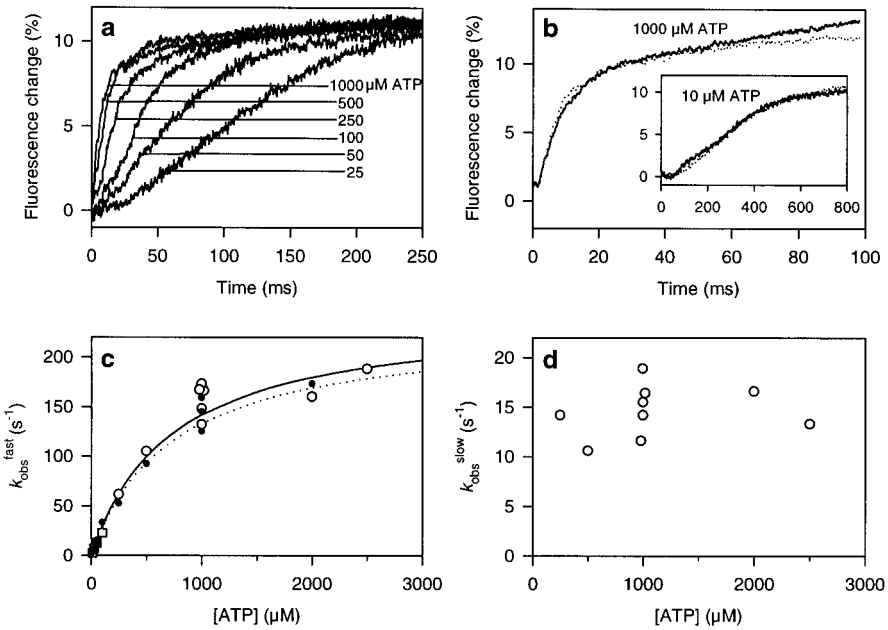

FIGURE 2: Myofibrillar tryptophan fluorescence transients in water: effects of ATP concentration and Ca^{2+}. (a) Transients in the absence of Ca^{2+} at different ATP concentrations. The reaction mixtures were 3 μM in myosin heads + ATP at the concentrations indicated. At ATP concentrations $\geq$250 μM, the transients were biphasic with kinetics $k^{Trp\ fast}$ and $k^{Trp\ slow}$. (b) Transients in the presence of Ca^{2+} (reaction mixture: 3 μM myosin heads + 1 mM ATP); the transient in the inset is an experiment at 10 μM ATP. In both cases, the transients in the absence of Ca^{2+} are plotted as dotted lines, for comparison. (c) ATP dependences of $k^{Trp\ fast}$: in the presence of Ca^{2+} (●) and in the absence of Ca^{2+} [(○) biphasic: $k^{Trp\ fast}$, (□) monophasic ignoring the lag: k_{obs}]. The data were fitted to hyperbolas giving $k^{Trp\ fast}{}_{max}$ and $K_{0.5}$, respectively: with Ca^{2+}, 230 ± 30 s^{-1} and 740 ± 140 μM (dotted line); with EGTA, 245 ± 20 s^{-1} and 730 ± 130 μM (continuous line). (d) ATP dependence of $k^{Trp\ slow}$ in the absence of Ca^{2+}. Mean value: 14.6 ± 2.4 s^{-1}. Conditions were as in Figure 1. For fitting procedure, see Materials and Methods.

Table 1: ATP-Induced Tryptophan and Pyrene Fluorescence Transients in Relaxed Myofibrils and S1: Effect of Solvent and Comparison with Chemical Kinetics (EGTA, 4 °C)[a]

	myofibrils			S1		
signal or process	water	ethylene glycol	methanol	water	ethylene glycol	methanol
tryptophan fluorescence						
rapid phase						
amplitude (%)	9.5 (±1.0)	5.7 (±0.4)	−4.4 (±0.6)	4 (±1)	2.6 (±0.2)	4.7 (±0.5)
$k^{Trp\ fast}{}_{max}$ (s^{-1})	230 (±20)	75 (±10)	37 (±4)	560 (±50)	450 (±50)	710 (±60)
initial slope ($\mu M^{-1}\ s^{-1}$)	0.25 (±0.02)	0.11 (±0.02)	0.23 (±0.04)	1.1 (±0.2)	0.44 (±0.05)	1.8 (±0.3)
slow phase						
amplitude (%)	3.2 (±0.2)	3.1 (±0.2)	3.2 (±0.5)	17 (±2)	10 (±2)	12 (±2)
$k^{Trp\ slow}{}_{max}$ (s^{-1})	15 (±3)	3.3 (±0.3)	8 (±2)	15 (±3)	3.1 (±0.5)	10 (±3)
ratio of ampl (fast/slow)	3.0	1.8	−1.4	0.24	0.26	0.4
chemical kinetics						
k_2/K_1 ($\mu M^{-1}\ s^{-1}$)	1.0 (±0.2)[b]	0.22 (±0.02)	nd	1.0 (±0.2)[b]	0.45 (±0.05)	nd
$k_3 + k_{-3}$ (s^{-1})	18 (±2)[b]	3.2 (±0.2)	nd	16 (±3)[b]	nd	nd
K_3	6.0 (±0.7)[b]	2.5 (±0.5)	nd	1.7 (±0.2)[b]	nd	nd
pyrene fluorescence						
amplitude (%)	9 (±1)	5 (±1)	−6 (±1)	−	−	−
$k^{Pyr}{}_{max}$ (s^{-1})	210 (±20)	71 (±7)	32 (±2)	−	−	−
initial slope ($\mu M^{-1}\ s^{-1}$)	0.28 (±0.02)	0.11 (±0.01)	0.18 (±0.05)	−	−	−

[a] Values are given as means (±SD) of different sets of experiments and may therefore slightly differ from the results shown in the figures. Chemical kinetics refer to cold ATP chase and P_i burst experiments. The buffers used are described under Materials and Methods. [b] From Herrmann et al. (*28*).

In the presence of Ca^{2+}, tryptophan fluorescence enhancement also occurred upon the addition of ATP to myofibrils (Figure 2b). However, whereas there was a lag phase and an exponential fast phase whose kinetics and amplitude were very similar to those found with relaxed myofibrils, a slow phase was difficult to interpret, presumably because the fluorescence signal was confounded by the myofibrillar shortening that occurs under this condition. The ATP dependence of the kinetics of the fast phase in the presence of Ca^{2+} is shown in Figure 2c; it is almost identical to that in its absence.

It is noteworthy that the kinetics of the fluorescent phases were considerably faster than the P_i release kinetics (k_4 in Scheme 1) whether or not the myofibrils were Ca^{2+}-activated [1.9 and 0.025 s^{-1}, respectively (*23*)]. Further, as the ATP concentration was increased, the total amplitude of the fluorescence signal remained constant which suggests that the final fluorescence state is independent of the ATP concentration (in the range 10 μM−4 mM).

Importantly, the initial slope of the dependence of $k^{Trp\ fast}$ upon the ATP concentration is only about one-fourth of k_2/K_1, i.e., the second-order binding constant for ATP (respec-

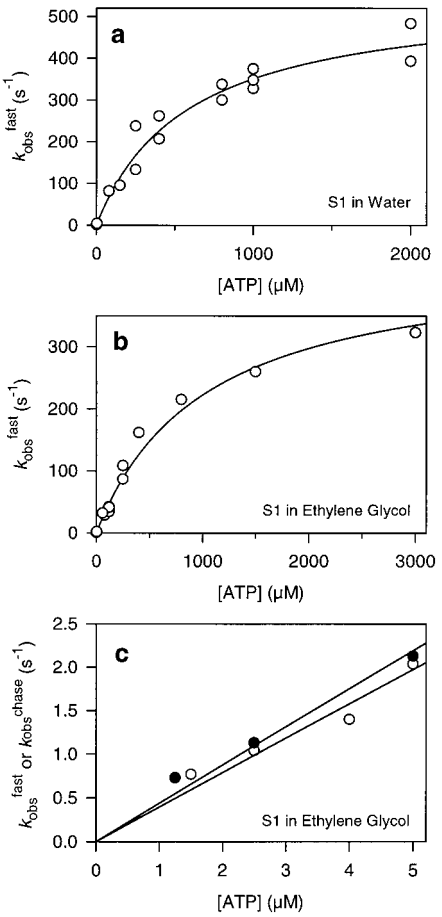

FIGURE 3: Dependences of the fast tryptophan fluorescence kinetics with S1 on the ATP concentration at 4 °C. For a typical transient, see Figure 8. (a) In water, the data were fitted to a hyperbola giving $k^{Trp\ fast}{}_{max} = 560 \pm 50\ s^{-1}$ and $K_{0.5} = 510\ \mu M$. (b) In 40% ethylene glycol, $k^{Trp\ fast}{}_{max} = 450 \pm 50\ s^{-1}$ and $K_{0.5} = 1$ mM. (c) Initial ATP dependence of $k^{Trp\ fast}$ (○) and cold ATP chase kinetics (●) in 40% ethylene glycol. The slopes of the dependences were 0.40 $\mu M^{-1}\ s^{-1}$ for the tryptophan fluorescence and 0.44 $\mu M^{-1}\ s^{-1}$ for the ATP chase.

tively 0.25 and 1 $\mu M^{-1}\ s^{-1}$, Table 1). This is different from the situation with isolated myosin heads which we now consider.

S1 Tryptophan Fluorescence Enhancement with ATP in Aqueous Buffer. Upon the addition of ATP to S1, there is an increase in fluorescence, a phenomenon that has been studied in several laboratories under different conditions (*15*, *17*, *19*, *27*). At high ATP, regardless of the conditions used, the signal is biphasic, and the kinetics of the initial phase are very rapid and therefore difficult to measure. Here, we carried out fluorescence stopped-flow experiments with S1 under our conditions (e.g., Figure 8a, top). Our results are in agreement with previous work, and we had sufficient time resolution to analyze the fast phase.

At low ATP, the kinetics of the fluorescence signal were monophasic: transient lag phases were not detected. As the ATP concentration was increased, the transient became biphasic, and we were able to measure the kinetics of the two phases (bursts) by $k^{Trp\ fast}$ and $k^{Trp\ slow}$.

The dependence of $k^{Trp\ fast}$ upon the ATP concentration is shown in Figure 3a, and the kinetic parameters obtained are in Table 1. Since the slope of the dependence is very close to that of the ATP chase kinetics (1.1 and 1.0 $\mu M^{-1}\ s^{-1}$, respectively; Table 1), this is further evidence that the fast fluorescence phase with S1 is a reflection of the ATP binding kinetics (K_1, k_2, Scheme 1). We note that our estimate for $k^{Trp\ fast}{}_{max}$ (i.e., k_2) of 560 s^{-1} is in good agreement with the 300−400 s^{-1} found by Johnson and Taylor (*15*) at high ATP (1 mM) and 5 °C, also by tryptophan fluorescence stopped-flow.

The $k^{Trp\ slow}$ is independent of the ATP concentration (not illustrated) at 15 s^{-1}, close to the $k_{obs} = 16\ s^{-1}$ measured in P_i burst experiments (*28*). Therefore, as found previously, the kinetics of the slow tryptophan fluorescence with S1 report the kinetics of the cleavage step, $k_3 + k_{-3}$ (formation of M**·ADP·P_i, Scheme 1).

That ATP binding on its own causes an increase in S1 fluorescence is supported by experiments with ADP which has the same effect (*27*). Here we find that ADP causes a total fluorescence increase of about 6% (results not illustrated), compared to a total of 21% with ATP (binding and cleavage; Table 1). Importantly, with myofibrils, whether Ca^{2+} was present or not, an increase in fluorescence could not be detected upon the addition of ADP (detection limit about 0.5%), even in the millimolar concentration range.

In conclusion, with S1, it appears that the fast tryptophan fluorescence transient reflects directly ATP binding. Also the ratios of the amplitudes of the phases (fast/slow) are very different for S1 and myofibrils (Table 1). Thus, with S1 most of the fluorescence signal occurs during the slow phase whereas with myofibrils it occurs during the fast phase.

Experiments with Pyrene-Labeled Myofibrils in Aqueous Buffer. Typical fluorescence transients with pyrene-labeled myofibrils (in the absence of calcium) are shown in Figure 4a,b together with tryptophan transients under the same conditions. At 15 μM ATP, both transients had lag and burst phases with similar kinetics. At 2 mM ATP, with pyrene-labeled myofibrils, the transient fits to a single exponential ($k^{Pyr} = 160\ s^{-1}$). The tryptophan transient of pyrene-labeled myofibrils was biphasic with $k^{Trp\ fast} = 170\ s^{-1}$ and $k^{Trp\ slow} = 18\ s^{-1}$. Importantly, unlike the biphasic tryptophan signal, there was no slow phase in the pyrene signal. The pyrene label had no significant effect on the kinetics of the tryptophan fluorescence enhancement (results not shown).

The dependences of k^{Pyr} and $k^{Trp\ fast}$ upon the ATP concentration are shown in Figure 4c, and as can be seen they are very similar. With the pyrene fluorescence, we find that $k^{Pyr}{}_{max} = 210\ s^{-1}$ and $K_{0.5} = 430\ \mu M$. At 20 °C, Ma and Taylor (*8*) found 830 s^{-1} and 280 μM, respectively.

Thus, it appears that the fast tryptophan and pyrene transients report the same phenomenon, probably cross-bridge detachment as suggested earlier for the pyrene fluorescence signal (*8*).

Effect of the Initial Myofibrillar Sarcomere Length on the Tryptophan Fluorescence Transients in Aqueous Buffer. If the fast phase of the tryptophan fluorescence enhancement transient reports some event at the thin filament−myosin head interface, then its amplitude should correlate with the degree of overlap of the myosin and actin filaments. Figure 5a shows tryptophan fluorescence transients obtained with myofibrils of average sarcomere lengths of 2.5 and 3.5 μm, prepared from fiber bundles under slack and prestretched conditions, respectively. The kinetics were very similar for

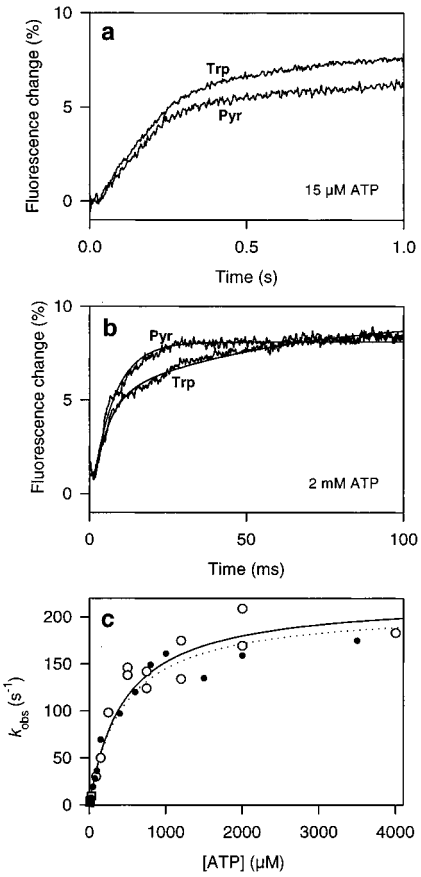

FIGURE 4: Tryptophan and pyrene fluorescence transients of pyrene-labeled relaxed (EGTA) myofibrils in water at 4 °C. The reaction mixtures were 3 μM in myosin plus 15 μM (a) or 2 mM ATP (b). In (a), both signals were fitted to a single exponential giving k_{obs} 4.3 s^{-1} (Pyr) and 3.8 s^{-1} (Trp). In (b), the pyrene signal was fitted to a single exponential ($k^{Pyr} = 160$ s^{-1}) and the tryptophan signal to two exponentials ($k^{Trp\ fast} = 170$ s^{-1}, $k^{Trp\ slow} = 18$ s^{-1}). (c) ATP dependence of k^{Pyr} (●) for pyrene fluorescence; k_{obs} (at low ATP, □) and $k^{Trp\ fast}$ (at high ATP, ○) for tryptophan fluorescence. In each case, the data were fitted to a hyperbola giving respectively for pyrene (dotted line) and tryptophan (continuous line) $k_{obs\ max} = 210 \pm 10$ and 220 ± 20 s^{-1}, $K_{0.5} = 430 \pm 70$ and 450 ± 100 μM.

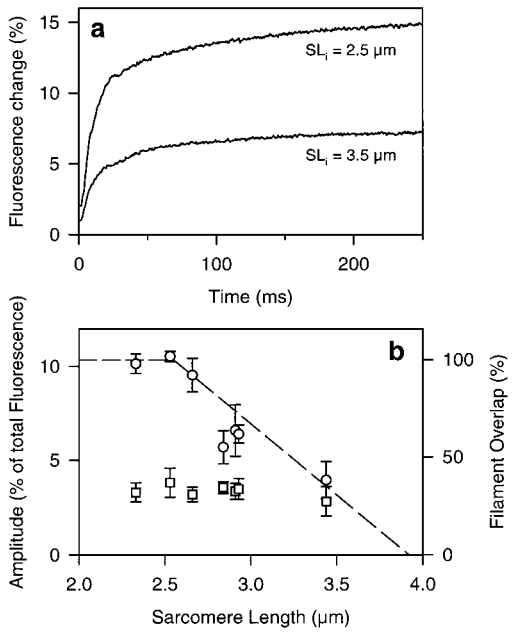

FIGURE 5: Fluorescence transients obtained at two initial myofibrillar sarcomere lengths, standard (2.5 μm) and prestretched (3.5 μm). In (a), the data were fitted to double exponentials: at 2.5 μm sarcomere length, the amplitude was $A^{Trp\ fast} = 11\%$, $k^{Trp\ fast} = 120$ s^{-1} and $A^{Trp\ slow} = 4\%$, $k^{Trp\ slow} = 11$ s^{-1}; at 3.5 μm sarcomere length, $A^{Trp\ fast} = 4\%$, $k^{Trp\ fast} = 121$ s^{-1} and $A^{Trp\ slow} = 3\%$, $k^{Trp\ slow} = 13$ s^{-1}. (b) Dependences of the amplitudes of the fast (○) and slow (□) phases on the initial sarcomere length. The dotted line represents the fraction of myosin heads overlapping with actin filaments calculated from the arrangements of the thick and thin filaments at different sarcomere lengths given in Woledge et al. (*54*) for mammalian muscle.

the two sarcomere lengths; however, it is noteworthy that the amplitude of the fast phase was much smaller with the myofibrils of the longer sarcomere length.

We show in Figure 5b that the amplitude of the fast fluorescence transient depends in an approximately linear manner on the extent of overlap, as calculated from the sarcomere length. Therefore, it appears that the myosin heads which are actin-free (in a nonoverlapping region) participate little or not at all with the fast fluorescence signal.

Myofibrils in 40% Ethylene Glycol. We now used another approach: solvent perturbation. By this means, we wished to slow the kinetic processes, especially those involved in ATP binding which were hard to study in water. Finally, we wished to obtain the kinetic processes under different sets of conditions to confirm and amplify their differences.

Because of its extensive use with muscle systems including myofibrils (*10* and references cited therein) and its ability to slow the kinetics of the initial steps of the Mg-ATPase of S1 and actoS1 (*29*), we first used 40% ethylene glycol as a perturbing agent. Further, it is difficult to investigate the myofibrillar transient burst kinetics in flow-quench studies at very low ATP concentrations (<10 μM) in aqueous buffer because of transient rigor activation of the myofibrillar ATPase. This phenomenon is not observed in the presence of 40% ethylene glycol, presumably because of the strong relaxing effects of this solvent (*10* and references cited therein).

Typical tryptophan fluorescence transients at different ATP concentrations are illustrated in Figure 6a. The results are qualitatively similar to those obtained in water (Figure 2). The dependences of $k^{Trp\ fast}$ and $k^{Trp\ slow}$ on the ATP concentration are shown in Figures 6b and 6c and the parameters obtained in Table 1.

Taking advantage of the effect of ethylene glycol in decreasing reaction rates, and especially its relaxation effect, we compared the kinetics of the chemical and fluorescent transients at a low ATP concentration (7.5 μM). The four transients are in Figure 7a: cold ATP chase (ATP binding) and P_i burst (cleavage step) kinetics compared with the kinetics of the tryptophan and pyrene fluorescence enhancements. As a first approximation, we fitted the data to a single exponential of kinetics k_{obs}, i.e., by ignoring the lag (as in water, above). We note that the kinetics of the two fluorescence and P_i burst transients are very similar. In particular, they all have similar lag phases followed by rapid rises whose kinetics were significantly slower than those of the ATP chase experiment. At all ATP concentrations tested (1−15 μM), both fluorescence transients and P_i burst had similar kinetics which were significantly slower than those of the cold ATP chase transients (Figure 7b).

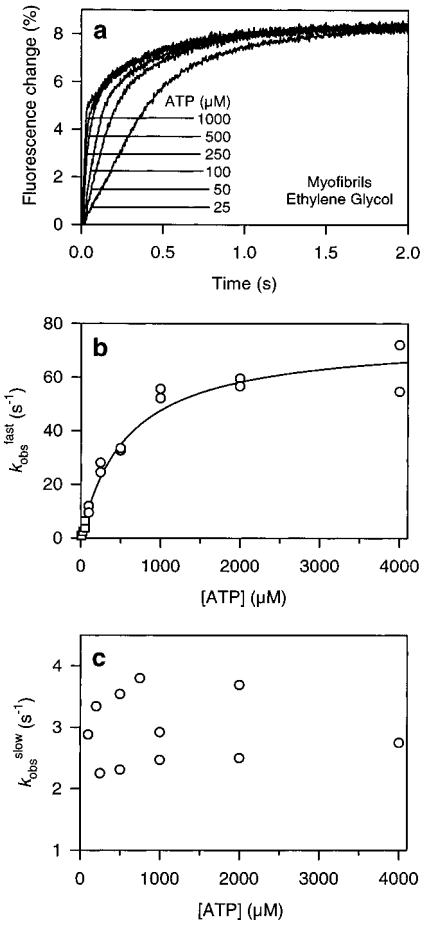

FIGURE 6: Relaxed myofibrillar tryptophan fluorescence transients in 40% ethylene glycol: effect of ATP concentration. The reaction mixtures were 3 μM in myosin heads + ATP at the concentrations indicated. (a) Transients recorded at different concentrations of ATP. At ATP concentrations $\leq$50 μM, the fluorescence enhancements were monophasic with observed rate constant k_{obs}. At higher [ATP], they were biphasic and gave $k^{Trp\ fast}$ and $k^{Trp\ slow}$ (see Figure 2). (b) Dependence of k_{obs} (low ATP, □) and $k^{Trp\ fast}$ (high ATP, ○) on the ATP concentration. The data were fitted to a hyperbola giving $k^{Trp\ fast}{}_{max} = 75 \pm 4\ s^{-1}$ and $K_{0.5} = 570 \pm 80\ \mu$M. (c) ATP dependence of $k^{Trp\ slow}$, with a mean value of $3.1 \pm 0.7\ s^{-1}$.

S1 in 40% Ethylene Glycol. As in water, the tryptophan fluorescence transients were biphasic at high ATP concentration with kinetics $k^{Trp\ fast}$ and $k^{Trp\ slow}$ (Figure 8b). $k^{Trp\ slow}$ was independent of the ATP concentration above 50 μM at 3.1 s^{-1}, very similar to the 3.3 s^{-1} found with myofibrils under the same conditions.

The dependence of $k^{Trp\ fast}$ on the ATP concentration is shown in Figure 3b (complete dependence: fluorescence stopped-flow only) and Figure 3c (low ATP concentrations: stopped-flow and cold ATP chase). A cold ATP chase experiment was also carried out at 100 μM ATP, and the k_{obs} obtained (50 s^{-1}, not illustrated) is in good agreement with the $k^{Trp\ fast}$ dependence. This agreement of the $k^{Trp\ fast}$ with the ATP chase kinetics confirms further that with S1, the fast fluorescence transient reports ATP binding. The kinetic parameters obtained in these experiments are summarized in Table 1.

Studies in 20% Methanol. The interest of this solvent is that its effects upon certain enzyme systems are different from those of ethylene glycol. In particular, in it, the myofibrillar ATPase is activated by Ca^{2+}, and there is

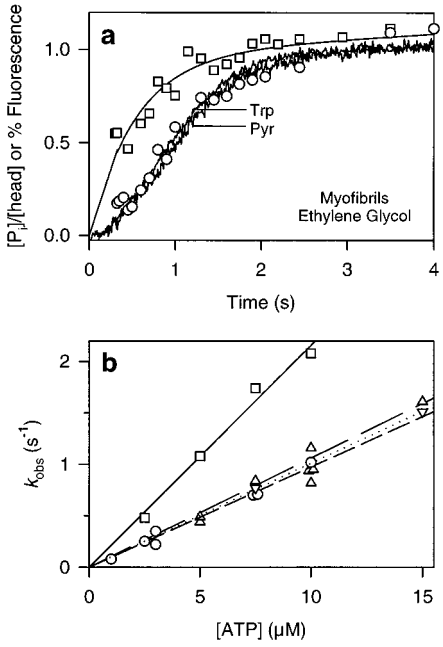

FIGURE 7: Comparison of the kinetics of fluorescence stopped-flow transients (tryptophan, pyrene) and rapid flow-quench transients (P_i burst, cold ATP chase) with relaxed myofibrils in 40% ethylene glycol at 4 °C. All the transient data were normalized to 1 to facilitate the comparison. (a) At 0.75 μM myosin heads + 7.5 μM ATP, the fluorescence curves are identical for tryptophan and pyrene and very similar to the P_i burst data (○). The k_{obs} obtained are in the range of $0.75 \pm 0.1\ s^{-1}$ for the three. The data for cold ATP chase (□) gave a $k_{obs} = 1.75 \pm 0.2\ s^{-1}$. The measured amplitudes of the transients were 12% (tryptophan signal), 4% (pyrene signal), 0.7 mol of P_i/mol of head (ATP chase), and 0.45 mol of P_i/mol of head (P_i burst). (b) Dependences of the k_{obs} on the ATP concentration for cold ATP chase (□), tryptophan fluorescence (△), pyrene fluorescence (▽), and P_i burst (○). The dependences were fitted by straight lines giving slopes of 0.22 $\mu M^{-1}\ s^{-1}$ for the ATP chase, 0.11 $\mu M^{-1}\ s^{-1}$ for the tryptophan fluorescence, 0.10 $\mu M^{-1}\ s^{-1}$ for the pyrene fluorescence, and 0.10 $\mu M^{-1}\ s^{-1}$ for the P_i burst. Conditions were as in Figure 1, and for further details, see Materials and Methods and Results.

shortening but only at temperatures above −2.5 °C (*9*). In ethylene glycol, there was neither Ca^{2+}-activation nor shortening except under special conditions (*10*). Further, with another ATP-handling enzyme, phosphoglycerate kinase, methanol, unlike ethylene glycol, increased significantly the substrate affinities (*30*).

In Figure 8 we show the effect of 20% methanol on the tryptophan fluorescence transients of myofibrils and S1 at a high ATP concentration. To compare, we also show the transients in water and 40% ethylene glycol. The transients were biphasic with both systems in all three solvents. However, methanol had the interesting effect of inverting the signal of the fast phase with myofibrils but not that of the slow phase. With S1, both phases remained positive. With myofibrils, the pyrene fluorescence transient was also inverted by methanol (result not illustrated). The effects of methanol upon the different transients are in Table 1. To summarize: in methanol, as in ethylene glycol and in water, whereas the kinetics of the fast phase of the tryptophan fluorescence enhancement are much faster with S1 than with myofibrils, the kinetics of the slow phase are very similar in the two systems. Further, the kinetics of the fast phase of myofibrillar tryptophan fluorescence are very close to those of pyrene fluorescence in all three solvents.

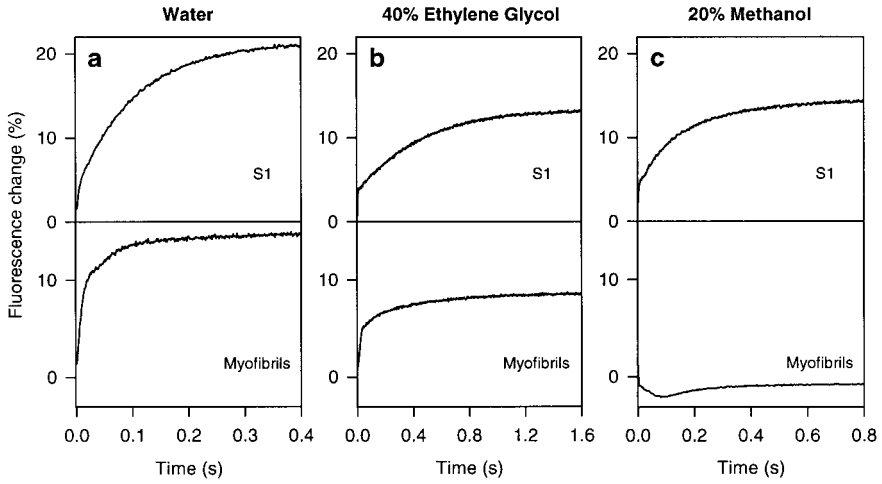

FIGURE 8: Comparison of the tryptophan fluorescence kinetics of S1 and myofibrils in different solvents at 4 °C. The reaction mixtures were 3 μM in myosin heads + 1 mM ATP, both for S1 (top panel) and for relaxed (EGTA) myofibrils (bottom panel). (a) no cosolvent; (b) 40% ethylene glycol; (c) 20% methanol. To facilitate comparison, the same time scales for both S1 and myofibrils were used. With S1, the fast phases were too rapid to be clearly seen on the plots. Conditions were as in Figure 1.

DISCUSSION

Under Results, we present kinetic data concerning the progression of the myofibril−ATP system (with the rigor complex A−M as the starting material) by following different signals: tryptophan and pyrene fluorescence by stopped-flow or P_i production by rapid flow-quench (P_i burst or cold ATP chase experiments). The studies were carried out under different conditions: large ATP concentration range, with or without Ca^{2+}, and with or without organic solvent. Our aim was, first, to exploit the fluorescence signal observed upon the addition of ATP to myofibrils. Second, it was to interpret the results obtained by a plausible scheme, based on previous works with S1 and, especially, actoS1. Finally, we wished to investigate the coupling between the ATPase cycle and cross-bridge attachment in the myofibril. Our strategy was to test different schemes by trying to fit them to our experimental results by simulation (see Materials and Methods). This was not easy, and finally, as discussed below, we chose Scheme 2 which is an extension of Scheme 1 by taking account of cross-bridge dissociation (defined by K_T). In an attempt at clarifying the terminology concerning the different states of the myosin heads with respect to actin (rigor, attached, detached, dissociated, associated), in Scheme 2 the heads are either *attached* or *detached*. In particular, with myofibrils, the heads are never "dissociated", which implies a release into solution, as with actoS1. This is a fundamental difference between actoS1 and myofibrils (and muscle fibers). In myofibrils, the heads are always in the vicinity of the thin filament, even if detached [for further arguments, see (*9*)]. In Scheme 2, attached states are indicated by A−M and detached states by A∼M.

Because of the better time resolution, we refer mainly to the data obtained in ethylene glycol. These data are qualitatively similar to those in water, despite there being little shortening in ethylene glycol (*10*).

Cold ATP Chase and Tight ATP Binding

By the *cold ATP chase* method, one measures specifically the kinetics of the tight binding of ATP to the myosin heads (see Materials and Methods): it is a way of obtaining the kinetics of an induced fit process. We have already shown that with myofibrils, whether relaxed (*28*), activated (*26*), or cross-linked chemically (*20*), k_{-2} (Scheme 2) is very small, as with actoS1 (*19*, *20*) and S1 (*24*). Therefore, we assume that the chase kinetics are defined entirely by K_1 and k_2. Unfortunately, because K_1 and k_2 are so large, it was impossible to obtain saturation in the chase kinetics, and under the conditions used here, only the second-order binding constant, k_2/K_1, was obtained. Despite the difference in starting material (A−M state with myofibrils, M alone with S1), k_2/K_1 values for S1 and myofibril are identical within experimental error in water (1 μM^{-1} s^{-1} at 4 °C, Table 1), but not identical in ethylene glycol (0.45 and 0.22 μM^{-1} s^{-1} respectively).

In the chase experiments, transient lag phases were not discerned under any condition used (different ATP concentrations, solvent composition, temperature) with any material tested (S1, actoS1, myofibrils). This confirms that the chase reports an early event on the ATPase pathways. It also shows that, at least in the millisecond time range, the ATP diffuses rapidly to the ATPase sites in myofibrils as for S1 (*6*, *26*).

Scheme 2

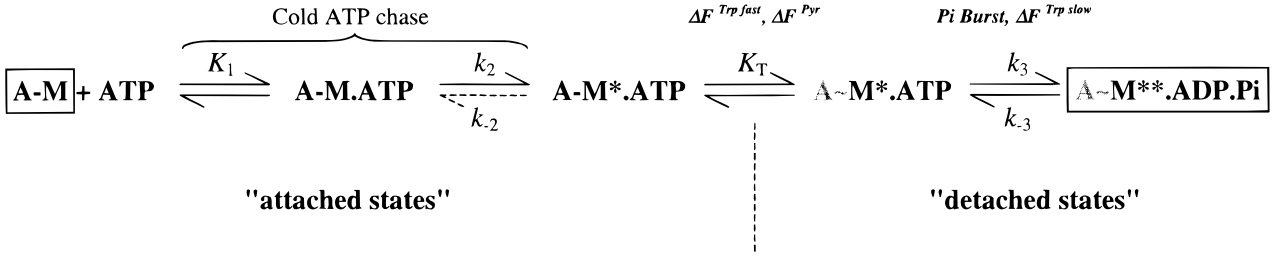

Analysis of the Fluorescence Data at High ATP Concentrations

These are the ATP concentrations at which the fluorescence curves become clearly biphasic: higher than 250 μM in water and 100 μM in ethylene glycol.

(A) Slow Tryptophan Fluorescence Phase and ATP Cleavage Step. Both in water (Figure 2d) and in ethylene glycol (Figure 6c), the kinetics of the slow tryptophan fluorescence phase are ATP-independent and within experimental error identical with either myofibrils or S1 (Table 1). This similarity between myofibrils and S1 may mean that with myofibrils ATP cleavage occurs in a detached state (A∼M), as first suggested for actoS1 (*2*). We discuss this further below. Under all conditions, the slow tryptophan fluorescence kinetics are close to those obtained at high ATP concentrations for $k_3 + k_{-3}$ in P_i burst experiments (Table 1). In addition to other arguments developed below, this means that the slow tryptophan fluorescence signal can be attributed unambiguously to step 3 in Scheme 2.

(B) Fast Tryptophan Fluorescence Phase. It is clear that the pyrene (ΔF^{Pyr}) and the fast tryptophan ($\Delta F^{Trp\ fast}$) fluorescence signals with myofibrils are kinetically very similar and therefore appear to report the same phenomenon. Since with actoS1 pyrene fluorescence perturbation reports the *dissociation* of actoS1 (*31*), we assume that the fast tryptophan fluorescence signal with myofibrils reports *detachment*, i.e., K_T in Scheme 2. We now compare the situation in myofibrils with those in S1 and actoS1.

(B, i) Comparison with S1. With S1 we also obtained biphasic tryptophan fluorescent transients at high ATP concentrations. The fast phase was dependent on the ATP concentrations in a hyperbolic manner (Figure 3a,b) and is attributed classically to the tight binding of the ATP, i.e., to the M·ATP⇔M*·ATP transition (Scheme 1). This situation is fundamentally different from that with myofibrils in which we attribute the fast tryptophan fluorescence signal (as the pyrene transient) to a change in the thin filament−head interface (A−M*·ATP⇔A∼M*·ATP, Scheme 2). Four arguments support this difference between the two systems.

First, consider the amplitudes of the fluorescence change in S1 and myofibrils. With S1 (as with actoS1), most of the signal reports the ATP cleavage, and the contribution of the first rapid phase to the overall signal is small (*14, 15, 17*, present study). In contrast, with myofibrils, it is the fast phase that dominates the overall fluorescence enhancement. We cannot exclude that a portion of this phase reports ATP binding but if so it would be very small and difficult to detect. Thus, if we assume that the amplitude of this putative phase is related to the amplitude of the slow phase as with S1 (Table 1), it would represent only about 1% of the total signal.

Second, 20% methanol inverted the polarity of the pyrene fluorescence and the fast phase of the tryptophan fluorescence signal with myofibrils whereas it did not affect the amplitude of the fast fluorescence signal with S1.

Third, when the initial filament overlap was reduced, the amplitude of the fast phase decreased (Figure 5), suggesting that in myofibrils the fast fluorescence signal reflects a change at the acto−myosin interface. The amplitude could extrapolate to 0 at 0% overlap. If so, this suggests that with myosin heads out of overlap, the increase of fluorescence due to ATP binding is very small.

Finally, upon mixing S1 with ADP, there was an increase of about 6% in tryptophan fluorescence, suggesting that the tryptophan fluorescence signal obtained reflects an ADP-induced isomerization of the myosin head. On the contrary, with myofibrils as with actoS1 (*32*) there was no change in fluorescence upon mixing with ADP, even in the millimolar concentration range.

(B, ii) Comparison with ActoS1. Three methods, based upon the stopped-flow, have been used to study the interaction of ATP with *actoS1*: light scattering, fluorescence of sensitive tryptophans in the S1, and fluorescence of pyrene-labeled actin. ActoS1 solutions are opaque, and upon addition of ATP, the light scattering decreases because the actoS1 dissociates. This method cannot be applied to myofibrils.

Millar and Geeves (*17*) showed that the actoS1 dissociation, as measured by light scattering at high ATP concentration, was faster than the tryptophan fluorescence transient which they propose reports ATP binding, as with S1. Previously, Johnson and Taylor (*15*) showed that there is a change in fluorescence when S1 binds to actin. This confirms the work of Biosca et al. (*19*), who showed that in ethylene glycol the kinetics of tight ATP binding (cold ATP chase) were slower than the dissociation (light scattering).

Pyrene-labeled actin in actoS1 is a sensitive and specific probe to study the actin−myosin interface. Geeves et al. (*33*) showed that upon the interaction of ATP with pyrene−actoS1 there is a fluorescent signal that reports an isomerization of a ternary actin−S1−ATP complex before a rapid dissociation. Therefore, with actoS1, pyrene fluorescence and light scattering give the same kinetics (*31*): they both report the dissociation process, which is faster than tight ATP binding as reported by tryptophan fluorescence.

In conclusion, as opposed to myofibrils, with actoS1, at least at high ATP concentrations, dissociation occurs with an early A−M·ATP complex, i.e., before the irreversible binding of ATP that finally gives the fluorescence signal when the S1 has been liberated. Further, with myofibrils, because of its large amplitude, it is unlikely that the fast phase reports a myosin head isomerization: with actoS1, the ratio of the amplitudes of the fast to the slow phase is typically 1:3 (*15, 33*) whereas with myofibrils it is 3:1, i.e., about 10 times higher than in actoS1. This suggests additional rapid tryptophan perturbations in myofibrils that cannot be explained merely by an isomerization of S1.

These fundamental differences between actoS1 and myofibrils are perhaps not surprising because in myofibrils, first, the myosin heads are organized in thick filaments, second, the actin is regulated, and, finally, actin is not "released" into solution but remains in the vicinity of the myosin heads (A∼M).

To summarize, with all three systems (S1, actoS1, and myofibrils), there is a fast fluorescence transient upon the addition of ATP. With S1 and actoS1, this transient is a reflection of ATP binding, but with myofibrils it appears to report head detachment.

Analysis of the Fluorescence Data at Low ATP Concentrations

We examine here experiments at ATP <15 μM where both chemical and fluorometric measurements are possible and

thus the kinetics comparable. Kinetically, the situation is particularly clear in ethylene glycol as illustrated in Figure 7 for experiments at 7.5 μM ATP. It is noteworthy that fluorescence (pyrene and tryptophan) and P_i burst experiments gave similar time courses, a lag phase followed by a fast burst phase, and that the kinetics of both are sensitive to the ATP concentration. The cold ATP chase gave unambiguously a kinetic constant $k_2[ATP]/K_1 = 1.65\ s^{-1}$, which is in the range of the kinetics of the lag phases in the other experiments.

At low ATP concentrations, we show that the ATP dependence of the fluorescence transient kinetics gave lower initial slopes than the ATP binding kinetics (about 1/4 in water and 1/2 in ethylene glycol, Table 1 and Figure 7b). Unfortunately, we could not compare the saturation kinetics of the two processes because it is very difficult to carry out ATP chase experiments with myofibrils above 100 μM ATP and thus to obtain individual values of k_2 and K_1. In Herrmann et al. (*28*), we showed that the dependence of the chase kinetics was linear up to 45 μM ATP in water (kinetics 40 s^{-1}), which suggests that $k_2 \gg 200\ s^{-1}$. From ATP chase experiments at *low* ATP concentrations (*28*), myofibrils and S1 have identical values for k_2/K_1 (1 $\mu M^{-1}\ s^{-1}$). If we assume that this identity remains at *high* ATP concentrations, then we can estimate k_2 for myofibrils from $k^{Trp}{}_{max}$ for S1: 400−500 s^{-1}, which is considerably faster than $k^{Trp\ fast}{}_{max} = 230\ s^{-1}$ (Table 1). We underline that in our experiments with myofibrils and S1 we used identical experimental conditions (here, and for example *23*, *28*).

In conclusion then, it appears that with myofibrils the chronology of events is as follows: ATP binding faster than cross-bridge detachment faster than ATP cleavage. This chronology is illustrated in Scheme 2 in which, as written, K_T describes an invariant, rapid equilibrium and the kinetics of the cleavage step ($k_3 + k_{-3}$) are implicitly independent of the ATP concentration. Despite several attempts (e.g., variants of the model, different values for the constants, etc.), we were unable to fit our data to this situation. The main difficulties are because, first, even at low ATP concentrations, the ATP-induced cross-bridge detachment rate is significantly slower than that of ATP binding (e.g., Figure 7b) and, second, the detachment kinetics depend over a significant range on the ATP concentration, becoming very fast at high [ATP] (e.g., Figure 6b) but probably not as fast as the ATP binding kinetics. Thus, the detachment kinetics cannot be explained simply by a slow isomerization step after ATP binding nor by a slow cross-bridge detachment step. Instead, we propose a model that is based upon Scheme 2 and which takes account the organization of the myofibril. The key to the model is that K_T is modulated by the proportion of the myosin heads in rigor.

Proposed Model for Cross-Bridge Detachment

Our model (Scheme 2) requires several assumptions. First, it is assumed that on the time scale of our experiments the cross-bridge attachment⇔detachment step is a rapid equilibrium with equilibrium constant K_T. There is evidence for this from Schoenberg et al. (*34*) and Kraft et al. (*35*), who proposed that in skinned rabbit psoas fibers in the presence of ATP or ATPγS, cross-bridges reversibly detach and reattach with rates much faster than the ATP binding kinetics. The second assumption is that ATP cleavage occurs only very slowly when the heads are associated (i.e., in the A−M*·ATP state): if not, the kinetics of the P_i burst would be faster than those of the dissociation at low [ATP], which was not observed (Figure 7). This assumption agrees with early work on actoS1 in which it was concluded that the kinetics of the cleavage step are slower in the associated than in the dissociated state (*16*); we discuss this further below.

Here our key assumption is that K_T (k_-/k_+, with k_- = cross-bridge detachment rate constant and k_+ = cross-bridge attachment rate constant) is modulated by R, the ratio of myosin heads in rigor to the total myosin heads. Thus, it is assumed that *during an experiment K_T changes* and that this change affects the detachment but not the ATP binding kinetics. At the beginning of an experiment, all heads are in a rigor state (A−M), so $R = 1$ and K_T is low. As more and more heads bind ATP, the proportion of rigor cross-bridges decreases, thereby increasing K_T. It was not possible to derive the detailed dependence of K_T upon R from our results. However, we were able to simulate the results both at high and at low ATP concentrations using either linear or hyperbolic dependences of k_+ and k_- upon R (see Materials and Methods for simulation procedure). To simulate the significant lags observed in the fluorescence transients, K_T had to change from $\ll 1$ at $R = 1$ ($t = 0$) to $\gg 1$ at $R = 0$ ($t = \infty$), with $K_T \approx 1$ at low fraction of rigor bridges (R = 0.1 and 0.3 in water and ethylene glycol, respectively). Using hyperbolic dependences, values used for k_+ and k_- were respectively 250 and 3000 s^{-1} at $R = 0$ ($t = \infty$) (*34*), and 5000 and 250 s^{-1} at $R = 1$ ($t = 0$). Values of k_2/K_1, K_3, k_3, and k_{-3} used for the simulations are in Table 1.

To conclude, we can explain our data by a K_T that is modulated by the proportion of myosin heads in rigor which changes during an experiment. Different related phenomena may explain this dependence of K_T upon the fraction of cross-bridges in rigor. First, consider the transient rigor activation of relaxed myofibrils that is observed at low ATP concentrations, even under multiturnover conditions (*36*, *37*). Thus, it could be that at low ATP concentrations, the regulatory system in the myofibril remains transiently activated by rigor activation, even in the absence of calcium, a situation which could affect K_T and thereby the fluorescence and ATP cleavage kinetics. Accordingly, the similarity of the fluorescence lag and burst kinetics in the presence and absence of Ca^{2+} suggests that Ca^{2+} activation does not change K_T. However, it could be that rigor activation shifts K_T toward actin-bound states more effectively than Ca^{2+}. This would be compatible with the finding that there is little effect of Ca^{2+} on the cross-bridge dissociation in the presence of ATP for S1 or HMM and regulated actin (*38*, *39*) or ATPγS and GTP for skinned fibers (*35*, *40*).

Second, a shift in K_T could be explained by *both* heads of myosin having to bind tightly ATP before cross-bridge detachment can occur and that there is some form of interaction between the heads. This could explain the delay of cross-bridge detachment kinetics upon ATP binding.

Finally, the shift could be due to a change in the structural arrangement of the actomyosin system in the myofibril, i.e., from the highly ordered state in rigor to a disordered orientation of the cross-bridges in relaxed or Ca^{2+}-activated myofibrils.

The interest of our model is that it takes account of the structural organization of the myofibril and, also, any communication that there might be between the myosin heads in a thick filament. Further, despite the complexity of these phenomena, the model can be summarized by a simple kinetic scheme.

Myofibrillar Cross-Bridges Detach Slower than ATP Binds: Implications

Our finding that the ATP binding kinetics (cold ATP chase) are faster than those of the cross-bridge detachment (pyrene and fast tryptophan fluorescent transients) is intriguing. First, it implies that second-order rate constants for ATP binding cannot be derived directly from methods reporting cross-bridge detachment kinetics, e.g., from the initial decay of force (*41), stiffness (42), linear dichroism (43), or change in intensities of equatorial reflections (44) upon flash photolysis of caged-ATP in muscle fibers.*

Second, our finding is in contrast with results with actoS1 where ATP-induced dissociation is faster than ATP binding [(*19*), confirmed by Millar and Geeves (*33*) and Tesi et al. (*45*)].

Schoenberg (*34*) estimated the rate of cross-bridge detachment in fibers. From the speed dependence of fiber stiffness under conditions similar to ours (ionic contents 0.16 M, 5 °C) and at 1 mM ATP, he obtained a rate of about 3000 s^{-1}, i.e., more than an order of magnitude faster than here with myofibrils (≈200 s^{-1}). How can this be explained? An important difference in the experimental procedures is that with Schoenberg, the ATP was present with the starting material; i.e., at $t = 0$, the predominant state was presumably A∼M**·ADP·P_i (*36*). Here the starting material was the rigor complex, A−M. It could be that when myofibrils are in the rigor state, they are brought out of this state only relatively slowly by ATP. Thus, there could be a relatively slow shift of attached to detached states.

Early cross-bridge models (*2*) postulated that the ATP cleavage is associated with the reversal of the power stroke, which thereby occurs in a detached configuration. With actoS1 at very high actin concentrations, the P_i burst is insignificant which is evidence that the ATP cleavage step is rate limiting when myosin is bound to actin (*16, 29, 46, 47*). Further, from experiments at intermediate concentrations of actin, Rosenfeld and Taylor (*16*) propose that in the attached state, the kinetics of the cleavage step are slower than in the detached state. Nevertheless, it has been difficult to decide whether cross-bridge detachment affects the kinetics of the cleavage step in an intact contractile system. Here, with myofibrils, we show that at low [ATP], the kinetics of the tryptophan and pyrene fluorescence transients are similar to the P_i burst kinetics, and that they are significantly slower than the ATP chase kinetics. *This suggests that cross-bridge detachment is required for ATP cleavage.* However, at saturating ATP concentrations, the P_i burst kinetics are much slower than those of the pyrene fluorescence and the fast phase of tryptophan fluorescence. Thus, at high [ATP], the cleavage kinetics are no longer limited by cross-bridge detachment rates but either by the cleavage itself or by a head isomerization immediately preceding cleavage.

Our finding that at low ATP concentrations the slower ATP-induced cross-bridge detachment and not the faster ATP binding limits ATP cleavage could explain certain unexpected results concerning the ATP dependences of the steady-state and transient rates of the myofibrillar ATPases. If at low ATP concentrations only the ATP binding were to be rate limiting for the formation of the A∼M**·ADP·P_i state, then $k_{cat}/K_m(\text{ATPase}) \approx k_2/K_1$ (since $k_{-2} \rightarrow 0$). However, with Ca^{2+}-activated myofibrils at 4 °C and ionic strength 0.16 M, $k_{cat}/K_m(\text{ATPase}) = 0.21\ \mu M^{-1}\ s^{-1}$ (*23*). This is much less than the $1.0\ \mu M^{-1}\ s^{-1}$ found for k_2/K_1 (*28*) but close to the $0.25\ \mu M^{-1}\ s^{-1}$ found by tryptophan fluorescence for the initial slope of $k^{Trp\ fast}$ upon [ATP] (under the same experimental conditions). Thus, the Michaelis−Menten kinetics of the myofibrillar steady-state ATPases may be determined not only by the ATP binding kinetics, but also, if not wholly, by the kinetics of the delayed ATP-induced cross-bridge dissociation.

ATP-Induced Tryptophan Fluorescence in Myofibrils: Origin of the Signal and Implications

Our discussion is with reference to the actoS1 model of Rayment et al. (*3*). With rabbit S1, the tryptophan residue that gives the ATP-induced fluorescence signals, i.e., both the fast and slow transients, is almost certainly Trp 510. Thus, in *Dictyostelium* myosin II, when Trp 501 (corresponding to Trp 510 in rabbit myosin) is replaced by a tyrosine residue, there is no longer a fluorescent signal upon the addition of ATP (*48*). Trp 510 is thus an intrinsic reporter group for S1; it is located in the lower 50 kDa domain.

With myofibrils, it is likely that Trp 510 in the myosin head is responsible for the slow fluorescent transient because its kinetics coincide with those of the P_i burst and they are similar to those with S1. However, it is unlikely that the same tryptophan can account fully for the fast phase of the fluorescence enhancement in myofibrils. First, whereas ADP gave a signal with S1, none could be detected with myofibrils. Second, with myofibrils the amplitude of the fast phase was considerably larger than with S1. Finally, the fast phase (but not the slow one) was affected in different ways by solvent perturbation. Thus, 20% methanol caused an inversion of the fast fluorescent transient with myofibrils but not with S1. So, which tryptophan residue(s) give(s) rise to the fast fluorescent transients with myofibrils?

Here we present evidence that the fast fluorescent transient with myofibrils is related to events at the thin filament−myosin head interface. This would explain the sensitivity of the phase to solvent perturbation. Therefore, we would expect the tryptophan residue(s) to be in a solvent-accessible and dynamic region at, or near, the thin filament−myosin head interface.

First, consider the tryptophan residues in the myosin head. Of these, Trp 131, which is located at the distal edge of the ATP binding pocket, is chemically the most reactive (*49, 50*) and, presumably, most accessible. Although this residue is unlikely to be involved in the tryptophan fluorescence enhancement with S1 (*50, 51*), its involvement cannot be excluded with the myofibril. Very recently Park et al. (*52*) suggested that the fluorescence of one or more of the remaining tryptophans on S1 (Trp 113, Trp 440, or Trp 595) is sensitive to ATP. Then, there are Trp 829 and Trp 831 that are in the long α-helical extension of the 20 kDa domain, beyond the regulatory light chain. These latter two tryptophans are not part of S1, and their implication would explain the large amplitude of the fast phase with myofibrils

compared with S1. However, we mainly favor a situation in which the sensitive tryptophan(s) is (are) in the actin not only because the kinetics of the pyrene reporter group (which is on the actin) and fast tryptophan transients are identical but also because the amplitudes of the transients are affected in the same way by solvent perturbation (Table 1). We note again that with S1, the amplitude of the fast fluorescence phase was unaffected by solvent. In actin the obvious candidates for the fast tryptophan fluorescence signal are Trp 340 and Trp 356, both of which are in, or close, to the thin filament−myosin head interface. Of course, we cannot exclude the possibility that the sensitive tryptophan is in another thin filament component. To identify the residues, further kinetic experiments coupled with chemical modification, site-directed mutagenesis, and solvent perturbation are needed.

CONCLUSIONS AND PROSPECTS

Here we exploited the ATP-induced intrinsic tryptophan fluorescence enhancement in myofibrils. The signal was large (13−14% of the total fluorescence) and rich in information. There were two components: a fast transient due to ATP-induced perturbation of the thin filament−myosin head interface and a slow transient due to the cleavage step, i.e., the formation of (A)M**·ADP·P_i states. There seems to be little advantage to label myofibrils with the extrinsic pyrene reporter group because the signal is no larger and, further, it does not report the formation of (A)M**·ADP·P_i states.

Our method could be useful to test different ATP analogues (NDP) for their effectiveness in inducing perturbations at the thin filament−myosin head interface and, in the same experiment, to determine the relative importance of the (A)M*·NTP and (A)M**·NDP·P_i states. For example, when GTP was added to myofibrils, there was a fluorescent signal which was monophasic with slower kinetics but an amplitude similar to that of the fast transient with ATP (R. Stehle, unpublished results), suggesting that with this analogue, the A∼M*·NTP state, accumulates rather than the A∼M**·NDP·P_i state as with ATP. The absence of a slow fluorescent transient with GTP makes sense because with this analogue and S1 intermediates of the type M*·GTP predominate and not M**·GDP·P_i as with ATP (*47*, *53*). Further the dependence of the amplitude upon the GTP concentration was Ca^{2+}-dependent which implies that with GTP the degree of myosin head detachment from the thin filament is Ca^{2+}-dependent as suggested by Frisbie et al. (*40*) for skinned fibers.

ACKNOWLEDGMENT

We are grateful to Patrick Chaussepied, Michael Geeves, and Gilles Divita for valuable discussions.

REFERENCES

1. Huxley, H. E. (1969) *Science 164*, 1356−1365.
2. Lymn, R. W., and Taylor, E. W. (1971) *Biochemistry 10*, 4617−4624.
3. Rayment, I., Holden, H. M., Whittaker, M., Yohn, C. B., Lorenz, M., Holmes, K. C., and Milligan, R. A. (1993) *Science 261*, 58−65.
4. Friedman, A. L., and Goldman, Y. E. (1996) *Biophys. J. 71*, 2774−2785.
5. Colomo, F., Piroddi, N., Poggesi, C., te Kronnie, G., and Tesi, C. (1997) *J. Physiol. (London) 500*, 535−548.
6. Sleep, J. A. (1981) *Biochemistry 20*, 5043−5051.
7. White, H. D. (1985) *J. Biol. Chem. 260*, 982−986.
8. Ma, Y. Z., and Taylor, E. W. (1994) *Biophys. J. 66*, 1542−1553.
9. Lionne, C., Stehle, R., Travers, F., and Barman, T. (1999) *Biochemistry 38*, 8512−8520.
10. Stehle, R., Lionne, C., Travers, F., and Barman, T. (1998) *J. Muscle Res. Cell Motil. 19*, 381−392.
11. Geeves, M. A. (1991) *Biochem. J. 274*, 1−14.
12. Trentham, D. R., Eccleston, J. F., and Bagshaw, C. R. (1976) *Q. Rev. Biophys. 9*, 217−281.
13. Chock, S. P., Chock, P. B., and Eisenberg, E. (1976) *Biochemistry 15*, 3244−3253.
14. Chock, S. P., Chock, P. B., and Eisenberg, E. (1979) *J. Biol. Chem. 254*, 3236−3243.
15. Johnson, K. A., and Taylor, E. W. (1978) *Biochemistry 17*, 3432−3442.
16. Rosenfeld, S. S., and Taylor, E. W. (1984) *J. Biol. Chem. 259*, 11908−11919.
17. Millar, N. C., and Geeves, M. A. (1988) *Biochem. J. 249*, 735−743.
18. Stehle, R., Lionne, C., Travers, F., and Barman, T. (1999) *J. Muscle Res. Cell Motil. 20*, 71−72.
19. Biosca, J. A., Barman, T. E., and Travers, F. (1984) *Biochemistry 23*, 2428−2436.
20. Herrmann, C., Sleep, J., Chaussepied, P., Travers, F., and Barman, T. (1993) *Biochemistry 32*, 7255−7263.
21. Knight, P. J., and Trinick, J. A. (1982) *Methods Enzymol. 85*, 9−12.
22. Herrmann, C., Lionne, C., Travers, F., and Barman, T. (1994) *Biochemistry 33*, 4148−4154.
23. Lionne, C., Travers, F., and Barman, T. (1996) *Biophys. J. 70*, 887−895.
24. Barman, T. E., and Travers, F. (1985) *Methods Biochem. Anal. 31*, 1−59.
25. Reimann, E. M., and Umfleet, R. A. (1978) *Biochim. Biophys. Acta 523*, 516−521.
26. Houadjeto, M., Travers, F., and Barman, T. (1992) *Biochemistry 31*, 1564−1569.
27. Bagshaw, C. R., and Trentham, D. R. (1974) *Biochem. J. 141*, 331−349.
28. Herrmann, C., Houadjeto, M., Travers, F., and Barman, T. (1992) *Biochemistry 31*, 8036−8042.
29. Biosca, J. A., Travers, F., Barman, T. E., Bertrand, R., Audemard, E., and Kassab, R. (1985) *Biochemistry 24*, 3814−3820.
30. Geerlof, A., Schmidt, P. P., Travers, F., and Barman, T. (1997) *Biochemistry 36*, 5538−5545.
31. Criddle, A. H., Geeves, M. A., and Jeffries, T. (1985) *Biochem. J. 232*, 343−349.
32. Trybus, K. M., and Taylor, E. W. (1982) *Biochemistry 21*, 1284−1294.
33. Geeves, M. A., Jeffries, T. E., and Millar, N. C. (1986) *Biochemistry 25*, 8454−8458.
34. Schoenberg, M. (1988) *Biophys. J. 54*, 135−148.
35. Kraft, T., Yu, L. C., Kuhn, H. J., and Brenner, B. (1992) *Proc. Natl. Acad. Sci. U.S.A. 89*, 11362−11366.
36. Lionne, C., Brune, M., Webb, M. R., Travers, F., and Barman, T. (1995) *FEBS Lett. 364*, 59−62.
37. Barman, T., Brune, M., Lionne, C., Piroddi, N., Poggesi, C., Stehle, R., Tesi, C., Travers, F., and Webb, M. R. (1998) *Biophys. J. 74*, 3120−3130.
38. Chalovich, J. M., Chock, P. B., and Eisenberg, E. (1981) *J. Biol. Chem. 256*, 575−578.
39. Wagner, P. D., and Giniger, E. (1981) *J. Biol. Chem. 256*, 12647−12650.
40. Frisbie, S. M., Chalovich, J. M., Brenner, B., and Yu, L. C. (1997) *Biophys. J. 72*, 2255−2261.
41. Goldman, Y. E., Hibberd, M. G., and Trentham, D. R. (1984) *J. Physiol. (London) 354*, 577−604.
42. Horiuti, K., Sakoda, T., and Yamada, K. (1992) *J. Muscle Res. Cell Motil. 13*, 685−691.
43. Tanner, J. W., Thomas, D. D., and Goldman, Y. E. (1992) *J. Mol. Biol. 223*, 185−203.

44. Poole, K. J., Rapp, G., Maeda, Y., and Goody, R. S. (1988) *Adv. Exp. Med. Biol. 226*, 391−404.
45. Tesi, C., Travers, F., and Barman, T. (1990) *Biochemistry 29*, 1846−1852.
46. Tesi, C., Barman, T., and Travers, F. (1990) *FEBS Lett. 260*, 229−232.
47. White, H. D., Belknap, B., and Webb, M. R. (1997) *Biochemistry 36*, 11828−11836.
48. Batra, R., and Manstein, D. J. (1999) *J. Biol. Chem. 380*, 1017−1023.
49. Peyser, Y. M., Muhlrad, A., and Werber, M. M. (1990) *FEBS Lett. 259*, 346−348.
50. Werber, M. M., Peyser, Y. M., and Muhlrad, A. (1987) *Biochemistry 26*, 2903−2909.
51. Hiratsuka, T. (1992) *J. Biol. Chem. 267*, 14949−14954.
52. Park, S., and Burghardt, T. P. (2000) *Biophys. J. 78*, 680a.
53. Eccleston, J. F., and Trentham, D. R. (1979) *Biochemistry 18*, 2896−2904.
54. Woledge, R. C., Curtin, N. A., and Homsher, E. (1985) *Monogr. Physiol. Soc. 41*, 1−357.

BI0004753